Bayesian Projection of COVID-19 Epidemic Trajectory

TIANSHU HUANG, PRANAV RAMA, ANTHONY VENTO, BRIAN TSANG, and JASON ZHANG, University of Texas at Austin

We present a novel interpretation of the SIR model in order to apply it to COVID-19, and use Bayesian Inference to estimate short-term epidemic curve trajectories and the true number of infectious cases. Finally, we show the efficacy of our posterior prediction by demonstrating that our prediction distribution matches the observed distribution in regions without significant interventions.

CCS Concepts: • **Mathematics of computing → Bayesian computation**; *Exploratory data analysis*; **Time series analysis**; *Metropolis-Hastings algorithm.*

Additional Key Words and Phrases: COVID-19, SIR Model, Epidemiology, Epidemic Curves

1 OVERVIEW

1.1 Dataset

Our data is sourced from an open-source project that aggregates COVID-19 epidemic curve data from a number of verified sources around the world [4]. The data consists of time-series curves documenting statistics such as the number of confirmed cases, deaths, recoveries, and population of various individual countries, states, and counties. The notation used to described this dataset is given in table 1.

As COVID-19 is known to spread in clusters [14], regions with low numbers of cases tend to have unstable trajectories. Therefore, we chose to only analyze regions with more than 50 confirmed cases for over 25 days.

The version of the dataset used for results described in this paper contains data up to April 24, 2020, and has a size of 32MB. In order to avoid "time travel" (using future information to test on the past), we split the data into a train set and a test set with the former containing data from March 30 to April 19 (21 days) and the latter holding data from April 20 to April 24 (5 days).

x_t	Confirmed cases on day t
$\boldsymbol{x}_{1:t}$	Confirmed cases on days $1-t$
X_t, $\boldsymbol{X}_{1:t}$	Random variable form of x_t and $\boldsymbol{x}_{1:t}$
y_t, $\boldsymbol{y}_{1:t}$, Y_t, $\boldsymbol{Y}_{1:t}$	Combined number of deaths and recoveries
N	Population of a location

Table 1. Notation used to describe data contained in our dataset

Authors' address: Tianshu Huang, tianshu.huang@utexas.edu; Pranav Rama, pranavrama9999@utexas.edu; Anthony Vento, anthony.vento@utexas.edu; Brian Tsang, briantsang2020@utexas.edu; Jason Zhang, jzhang27143@utexas.edu, University of Texas at Austin, Austin, Texas.

1.2 Goals

Our focus and guiding philosophy centers around explainability from the standpoint of an ordinary citizen. Therefore, our priorities are, in order:

(1) Explainability, as parameters with real-world interpretations
(2) Verifiability, in the sense of a posterior distribution
(3) Absolute accuracy

To that end, the primary goal of our work is to measure hidden COVID-19 population dynamics. Specifically, we seek to estimate the number of infective cases, which is thought to mostly consist of asymptomatic and presymptomatic cases. Our secondary goal is to predict the future number of cases, which we use to verify the validity of our methodology.

2 SIR MODEL

2.1 Overview

The Susceptible-Infected-Removed (SIR) model is a conventional compartmental method used to model the dynamics of an infectious disease. This model is based on three parameters: an infection rate β, a removal rate γ, and a fixed population size N. Over a series of discrete time intervals, the SIR model partitions a population into susceptible ($\boldsymbol{S}$), infected ($\boldsymbol{I}$), and removed ($\boldsymbol{R}$) states, where the removed state usually refers to deaths and recovered cases. The population dynamics of this model are determined by the following system of differential equations:

$$\begin{aligned} \frac{d\boldsymbol{S}}{dt} &= -\frac{\beta \boldsymbol{I}\boldsymbol{S}}{N} \\ \frac{d\boldsymbol{I}}{dt} &= \frac{\beta \boldsymbol{I}S}{N} - \gamma \boldsymbol{I} \\ \frac{d\boldsymbol{R}}{dt} &= \gamma \boldsymbol{I} \end{aligned} \tag{1}$$

We will refer to the solved differential equations given the appropriate initial conditions and parameter as

$$\boldsymbol{S}(t), \boldsymbol{I}(t), \boldsymbol{R}(t) = SIR(t; \beta, \gamma, S_0, I_0, R_0, N) \tag{2}$$

which we will shorten to $SIR(t; \beta, \gamma)$ or $SIR(t; \beta, \gamma, I_0)$.

In epidemic models, the basic reproduction number R_0 is a critical statistic that estimates the average number of new infections from an infected individual. An SIR model estimates R_0 as β/γ. Since the SIR model is deterministic in β and γ, fitting an SIR model reduces to finding optimal values of β and γ given time-series data. Traditionally, data for a disease's confirmed cases are treated as observations of $\boldsymbol{I}$ [5].

2.2 Fitting SIR

There are two general approaches to fitting the SIR model: minimizing an objective function, and Bayesian inference.

2.2.1 SIR using Objective Functions. Objective function minimization such as minimizing mean square error is commonly used [2, 10–12]. This method is simple, easy to implement, and easily explainable from a methodology standpoint. However, it has several weaknesses that inhibit explainability of the results:

- **Manual Balancing**: If optimizing MSE to fit a cumulative case curve, later data points will be given a larger weight than earlier cases, which should be adjusted. Similarly, if fitting MSE on both confirmed cases and deaths (around $1/20$ compared to cases), the weight given to the MSE of confirmed deaths must be manually increased.
- **No Uncertainty**: While the value of the objective function can be provided at the values computed, this does not directly translate into a confidence interval or other actionable or comparable value.
- **No Soft Prior**: Prior assumptions can inform weights and normalization, but these impositions are not 'soft' — the model cannot choose to ignore them.

2.2.2 SIR using Bayesian Inference. The other major technique used to fit SIR models is Bayesian Inference. This method is also very popular [1, 16]. Due to its inherent explainability, we believe Bayesian Inference is much better suited for public health and epidemiological applications, where exact predictions can be much less important than explainable predictions with quantifiable error. A common formulation of Bayesian SIR is as follows:

$$\begin{aligned} B &\sim \text{Gamma}(2,2) \\ \Gamma &\sim \text{Gamma}(2,2) \\ [\boldsymbol{S}(t), \boldsymbol{I}(t), \boldsymbol{R}(t) | B, \Gamma] &\sim \text{Poisson}(SIR(t; B, \Gamma)) \end{aligned} \tag{3}$$

Here, the initial conditions are set as $\boldsymbol{S}(0) = N - X_0 - Y_0$, $\boldsymbol{I}(0) = X_0$, and $\boldsymbol{R}(0) = Y_0$ for total population N, active cases X, and combined deaths and recoveries Y.

Since $\boldsymbol{I}$ and $\boldsymbol{R}$ are observed, this leads to the posterior formulation

$$\begin{aligned} p(B, \Gamma | \boldsymbol{I}(1:t), \boldsymbol{R}(1:t)) &\propto p(\boldsymbol{I}(1:t), \boldsymbol{R}(1:t) | B, \Gamma) p(B, \Gamma) \\ &= p(\boldsymbol{I}(1:t) | B, \Gamma) p(\boldsymbol{R}(1:t) | B, \Gamma) p(B, \Gamma) \\ p(\boldsymbol{I}(1:t) | B, \Gamma) &= \prod_{n=1}^{t} \text{Poisson}(\boldsymbol{I}(n); SIR(n; B, \Gamma) \\ p(\boldsymbol{R}(1:t) | B, \Gamma) &= \prod_{n=1}^{t} \text{Poisson}(\boldsymbol{R}(n); SIR(n; B, \Gamma)) \\ p(B, \Gamma) &= \text{Gamma}(B; 2, 2) \text{Gamma}(\Gamma; 2, 2) \end{aligned} \tag{4}$$

2.3 Weaknesses of Conventional SIR

The SIR model as typically applied to COVID-19 is based on a few key assumptions [9]:

(1) Recovery grants immunity for a significant amount of time
(2) The transmission characteristics β and γ are time-independent
(3) All infected people have similar characteristics, and all susceptible people have similar characteristics
(4) The number of infective people can be measured through testing

While so far there is no evidence against assumption (1), rampant under-testing and the wide variety of policy interventions suggest that (2), (3), and (4) are invalid.

The impact of these false assumptions can be seen by applying the conventional SIR model (Equation 3, Equation 4), where $\hat{\beta}$, $\hat{\gamma}$ and $\hat{R}_0$ values are obtained that are not consistent with reality (Appendix A).

2.4 Proposed Solutions

Proposed solutions to address the weaknesses of conventional SIR fall into three general categories:

(1) **Increased granularity in S**: split susceptible cases into different categories depending on whether they are in self-isolation or otherwise quarantined [8]
(2) **Increased granularity in I**: split infective cases into different categories depending on whether they have tested positive or not [3, 17]
(3) **Add time-dependence**: allow β and γ to vary over time [3]

All solutions involve the addition of new parameters and/or states, which reduces explainability. Therefore, in order to preserve explainability while also addressing weaknesses of SIR, we propose a solution that is equivalent to a different perspective of (2), but avoids adding new states.

3 METHODOLOGY

3.1 Our Interpretation of SIR

In order to address some of the weaknesses of SIR described above, we propose the following interpretation of the SIR assumptions when applied to COVID-19:

- The number of infectious people $\boldsymbol{I}(t)$ is hidden
- Once a person becomes a confirmed case, they are quarantined or stay in self-isolation, and are no longer infective; $\boldsymbol{R}(t) = X_t$.

Since the model does not add new states, it is simpler and more explainable than the methods described above. However, our model still retains the ability to estimate the true number of infections states like [3, 17].

In order to apply Bayesian Inference on our model, we require the introduction of a new parameter, $\boldsymbol{I}(0) = I_0$ to the base Bayesian SIR model (Equation 3):

$$\begin{aligned} B &\sim \text{Gamma}(2,2) \\ \Gamma &\sim \text{Gamma}(2,2) \\ I_0 &\sim \text{Poisson}(\boldsymbol{R}(5) - \boldsymbol{R}(0)) \\ [\boldsymbol{S}(t), \boldsymbol{I}(t), \boldsymbol{R}(t) | B, \Gamma] &\sim \text{Poisson}(SIR(t; B, \Gamma)) \end{aligned} \tag{5}$$

The constant initial conditions are therefore modified to be $\boldsymbol{S}(0) = N - \boldsymbol{I}(0) - \boldsymbol{R}(0) = N - X_0 - \boldsymbol{I}(0) \approx N - I_0$ and $\boldsymbol{R}(0) = X_0$.

The posterior is therefore modified to be

$$\begin{aligned} p(B, \Gamma, I_0 | \boldsymbol{R}(1:t)) &\propto p(\boldsymbol{R}(1:t) | B, \Gamma, I_0) p(B, \Gamma, I_0) \\ p(\boldsymbol{R}(1:t) | B, \Gamma, I_0) &= \prod_{n=1}^{t} \text{Poisson}(\boldsymbol{R}(n); SIR(n; B, \Gamma, I_0)) \\ p(B, \Gamma, I_0) &= \text{Gamma}(B; 2, 2) \text{Gamma}(\Gamma; 2, 2) \\ &\quad \text{Poisson}(I_0; \boldsymbol{R}(5) - \boldsymbol{R}(0)) \end{aligned} \tag{6}$$

Since the incubation period of COVID-19 is anecdotally known to be about 5 days, we reason that most infective cases on day 0 ($\boldsymbol{I}(0)$) will have become new cases by day 5. Therefore, we use $\boldsymbol{R}(5) - \boldsymbol{R}(0)$, the number of new cases for the first 5 days, as our prior mean.

3.2 Inference

In order to perform Bayesian Inference on the model (*Equation* 5), we apply MCMC, which we implemented using pymc3 [15]. Specifically, we use the "No U-Turn Sampler" (NUTS) [6], a Hamiltonian Monte-Carlo technique, on the continuous B and Γ, and generic Metropolis-Hastings [13] on the discrete I_0.

For our best estimate, we used $\hat{\beta}, \hat{\gamma}, \hat{I}_0 = E[B, \Gamma, I_0 | \boldsymbol{R}(1:t) = \boldsymbol{x}_{1:t}]$ since we experimentally determined that the posteriors were largely outlier-free.

For each inference, we discarded the first 500 samples as burn-in, and kept the remaining 500. Throughout our sampling, we were able to observe that B, Γ, and I_0 mixed well, and were not dominated by our priors.

3.3 Projection

In order to perform projection, we need to take into account two sources of variability: variability induced by $p(B, \Gamma, I_0 | \boldsymbol{R}(1:t) = \boldsymbol{x}_{1:t})$, and variability due to $p(\boldsymbol{R}(t) | B, \Gamma, I_0)$.

$p(B, \Gamma, I_0 | \boldsymbol{R}(1:t) = \boldsymbol{x}_{1:t})$ is simple to account for; instead of projecting just the mean, we propagate all (B, Γ, I_0) samples through SIR. On the other hand, $p(\boldsymbol{R}(t) | B, \Gamma, I_0)$ is a bit more tricky. Since our model sets the likelihood $p(\boldsymbol{R}(t) | B, \Gamma, I_0)$ a priori (Equation 5), and does not learn it from the data, it is inappropriate to apply our model directly.

Instead, we sample this noise using a bootstrapped approach from the observed data. Consider the conditional deviation from the mean

$$\begin{aligned} p(\mathcal{E} | B, \Gamma, I_0) &= p(\boldsymbol{R}(T+1) - \boldsymbol{R}(T) - E[\boldsymbol{R}(T+1) - \boldsymbol{R}(T) | B, \Gamma, I_0]) \\ &= p([\boldsymbol{R}(T+1) - \boldsymbol{R}(T)] \\ &\quad - [SIR(T+1; B, \Gamma, I_0) - SIR(T; B, \Gamma, I_0)]) \end{aligned} \tag{7}$$

Assuming that $\mathcal{E}$ is time-independent, $\mathcal{E} \sim p(\mathcal{E} | B, \Gamma, I_0)$ can be sampled by setting $T \sim \text{Unif}(0, t)$. Each $[\mathcal{E} | B, \Gamma, I_0]$ was sampled 10 times, which combined with the 500 samples of (B, Γ, I_0) resulted in 5000 samples total for each projection.

3.4 Validation

In order to validate our projected 5-day new confirmed case distribution $D = \boldsymbol{R}(t+5) - \boldsymbol{R}(t)$, we use the fact that for any continuous random variable X,

$$F_X(X) \sim \text{Unif}(0, 1) \tag{8}$$

Since D are all relatively large ($\gg 100$), we treat D as a continuous random variable, and evaluate $F_D(d)$ for $d = x_{t+5} - x_t$, and compare to a Unif(0, 1) using the Kolmogorov-Smirnov goodness-of-fit test [7] with a rejection threshold of 0.05.

Since many regions had extreme variations in confirmed case numbers at the end of our training period or during the validation period (typically triggered by extreme policy or testing changes), we ignored countries with $F_D(d) > 0.99$ or $F_D(d) < 0.01$. While this does remove outliers that would affect $F_D(d)$, since d varies continuously, any deviations from the uniform distribution will still manifest as points with $F_D(d)$ close to 0 and 1.

Country	$\hat{\beta}$	$\hat{\gamma}$	$\hat{\beta}/\hat{\gamma}$	$\hat{I}_t$	$1000\hat{I}_t/N$
France	0.236	0.200	1.179	47208	0.703
Belgium	0.235	0.248	0.949	4507	0.394
United States	0.261	0.259	1.007	116728	0.359
Turkey	0.292	0.250	1.166	27838	0.339
Netherlands	0.247	0.245	1.006	4380	0.256
Spain	0.213	0.262	0.812	9032	0.193
Italy	0.239	0.258	0.925	10785	0.179

Table 2. Sample estimated country parameter values

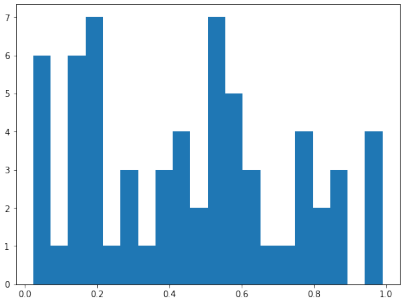

Fig. 1. Overall $F_D(D)$ distribution for Country Projection

4 RESULTS

We applied our Bayesian Projection methodology to 104 countries and counties in 8 US states. Additional plots not shown here can be seen in Appendix B.

4.1 Countries

4.1.1 SIR Parameter Estimates. We applied our methodology to 104 countries with at least 50 cases for 25 days. Sample values for $\hat{\beta}, \hat{\gamma}, R_0 = \hat{\beta}/\hat{\gamma}, \hat{I}_t$, and $1000\hat{I}_t/N$ are recorded in Table 2.

These values are consistent and match with our expectations. In all countries, we obtained a $R_0 = \hat{\beta}/\hat{\gamma}$ value of between 0.8 and 1.2, which is consistent with these countries' confirmed cases growing at a largely linear rate, with some countries growing faster or slower. We also obtained typical $\hat{\gamma}$ values of around 1/3 to 1/5, which corresponds to a removal time of 3 to 5 days once infectious. This is also consistent with typical testing time frames, and the anecdotal 5-day typical incubation period described previously.

4.1.2 Sample Results. Estimated mean trajectories and 5-day new case projection distributions for the United States, Germany, Canada, and Italy are shown in Figure 4 and Figure 5.

4.1.3 Projection. As a whole, we applied our evaluation methodology (Equation 7) to the set of countries, and obtained a $F_D(D)$ distribution histogram (Figure 1) that looks largely uniform, and corresponds to a Kolmogorov-Smirnov test p-value of 0.139.

4.2 US States

4.2.1 Sample Parameter Estimates for New York and Texas. We applied our methodology to counties in 8 US States. Sample values for

County	City	$\hat{\beta}$	$\hat{\gamma}$	$\hat{\beta}/\hat{\gamma}$	$\hat{I}_t$	$1000\hat{I}_t/N$
Richmond	NYC	0.286	0.264	1.083	1759	3.695
Bronx	NYC	0.251	0.249	1.008	4265	3.008
Westchester	NYC	0.251	0.256	0.983	2413	2.495
Nassau	NYC	0.263	0.272	0.968	3365	2.480

Table 3. Sample estimated New York parameter values

County	City	$\hat{\beta}$	$\hat{\gamma}$	$\hat{\beta}/\hat{\gamma}$	$\hat{I}_t$	$1000\hat{I}_t/N$
Harris	Houston	0.363	0.320	1.134	1290	0.274
Travis	Austin	0.266	0.242	1.097	265	0.208
Tarrant	Dallas	0.245	0.215	1.141	385	0.183
Fort Bend	Houston	0.334	0.314	1.063	137	0.170

Table 4. Sample estimated Texas parameter values

State	K-S p-value	State	K-S p-value
New York	0.032	California	0.950
Pennsylvania	0.180	Colorado	0.324
Florida	0.739	Washington	0.238
New Jersey	0.000	Texas	0.069

Table 5. Kolmogorov-Smirnov test results for US States

$\hat{\beta}, \hat{\gamma}, R_0 = \hat{\beta}/\hat{\gamma}, \hat{I}_t$, and $1000\hat{I}_t/N$ for counties in New York and Texas are recorded in Table 3 and Table 4, respectively. Mean trajectories could not fit in the 4-page limit and are available on request.

4.2.2 Projection. We also applied our evaluation methodology (Equation 7) to counties in 8 US states, and obtained a $F_D(D)$ distribution histogram for each state (Figure 3). For each state, we reported a Kolmogorov-Smirnov p-value shown in Table 5. For some states such as California ($p = 0.950$), our model performed very well. On the other hand, New York and New Jersey have p-values of < 0.05. After examining the 5 day validation period, we saw that New York and New Jersey had a general decline in new cases at the end of the training period and throughout the validation period which our model could not predict.

5 DISCUSSION

As of 5/1, Texas has committed to reopening some businesses in an effort to try to get the state back to normal operation. Is this a good idea?

First, the number of infective cases per thousand, $1000\hat{I}_t/N$, is 10 times lower in Texas than in New York, so Texas is likely in no imminent danger of runaway infections, and hospitals in Texas are not in danger of being overwhelmed.

However, examining our comparison of New York and Texas, we can observe that $\hat{\beta}$ and $\hat{\gamma}$ values for Texas are generally higher than that of New York. This indicates that while testing is more effective in Texas than New York, social distancing measures in Texas are less effective. This is one of the theoretical consequences of the SIR model: the basic reproduction number $R_0 = \beta/\gamma$ can be decreased by either decreasing infectiousness β through social distancing measures or increasing the removal rate γ by increasing testing.

For our final answer, we examine trends in $\hat{I}_t$. In Figure 6, we can see that several counties have a general downwards trend in the infectious population, many counties have an increasing number of infectious people. Therefore, we conclude that as of 4/24, only some counties should reopen, and Texas as a whole should *not* relax social distancing measures.

6 FUTURE WORK

Based on our experience with the described methodology, we suggest modelling the state transitions $\frac{dR}{dt}$ as Poisson instead of modelling the cumulative number of cases. Ordinarily, instability in the day-to-day case numbers makes the cumulative curve preferable to the marginal curve; however, the flexibility of Bayesian inference makes direct comparison possible.

Next, we do not recommend using pymc3. The library is extremely slow, and features a global lock which prevents parallel computing despite being unable to use multiple computing cores. Therefore, for future work on this problem, we would need to implement our own MCMC sampler. Following a more effective implementation of MCMC, we propose the following problems:

- **Intervention Evaluation**: For every possible 14-day train and 7-day test interval, fit our model. If our projection is significantly different from observed values, an intervention may have occurred. Do these changes correspond to a policy intervention? Conversely, do policy interventions lead to deviations from our model prediction?
- **Anomaly Detection**: Apply our model to all regions in the dataset. For each large region, consider all sub-regions as a population, and find outliers based on the estimated $\hat{\beta}$ and $\hat{\gamma}$. Do these outliers have reasonable explanations?

7 CONCLUSION

Using Bayesian inference based on a reinterpretation of SIR, we have successfully obtained posterior distributions for new case numbers in countries without major interventions, and used this to justify our estimates of the number of infective cases over time. We have applied our methodology to US states with large numbers of cases, and obtained favorable results for 6 out of 8 states attempted. Finally, we applied our method to Texas in order to conclude that while many counties in Texas can reopen, Texas as a whole should not relax social distancing measures.

REFERENCES

[1] Cristian Bayes, Victor Sal y Rosas, and Luis Valdivieso. 2020. Modelling death rates due to COVID-19: A Bayesian approach. arXiv:stat.AP/2004.02386

[2] Giuseppe C. Calafiore, Carlo Novara, and Corrado Possieri. 2020. A Modified SIR Model for the COVID-19 Contagion in Italy. arXiv:arXiv:2003.14391

[3] Yi-Cheng Chen, Ping-En Lu, Cheng-Shang Chang, and Tzu-Hsuan Liu. 2020. A Time-dependent SIR model for COVID-19 with Undetectable Infected Persons. arXiv:q-bio.PE/2003.00122

[4] Larry David. 2020. Corona Data Scraper. https://coronadatascraper.com

[5] Jonathan Fintzi, Xiang Cui, Jon Wakefield, and Vladimir N. Minin. 2016. Efficient data augmentation for fitting stochastic epidemic models to prevalence data. arXiv:stat.CO/1606.07995

[6] Matthew D. Hoffman and Andrew Gelman. 2011. The No-U-Turn Sampler: Adaptively Setting Path Lengths in Hamiltonian Monte Carlo. arXiv:stat.CO/1111.4246

[7] Frank J. Massey Jr. 1951. The Kolmogorov-Smirnov Test for Goodness of Fit. *J. Amer. Statist. Assoc.* 46, 253 (1951), 68–78. https://doi.org/10.1080/01621459.1951.10500769

[8] Xavier Rodó Leonardo López. 2020. A modified SEIR model to predict the COVID-19 outbreak in Spain and Italy: simulating control scenarios and multi-scale epidemics. https://www.medrxiv.org/content/10.1101/2020.03.27.20045005v3.full.pdf+html

[9] Alun Lloyd and Lorenzo Pellise Mick Roberts, Viggo Andreasen. 2014. Nine challenges for deterministic epidemic models.

[10] Babacar Mbaye Ndiaye, Lena Tendeng, and Diaraf Seck. 2020. Analysis of the COVID-19 pandemic by SIR model and machine learning technics for forecasting. arXiv:q-bio.PE/2004.01574

[11] Igor Nesteruk. 2020. Estimations of the coronavirus epidemic dynamics in South Korea with the use of SIR model. https://doi.org/10.13140/RG.2.2.15489.40807

[12] Jonathan M Read, Jessica RE Bridgen, Derek AT Cummings, Antonia Ho, and Chris P Jewell. 2020. Novel coronavirus 2019-nCoV: early estimation of epidemiological parameters and epidemic predictions. *medRxiv* (2020). https://doi.org/10.1101/2020.01.23.20018549

[13] Christian P. Robert. 2015. The Metropolis-Hastings algorithm. arXiv:stat.CO/1504.01896

[14] Hagai Rossman, Ayya Keshet, Smadar Shilo, Amir Gavrieli, Tal Bauman, Ori Cohen, Esti Shelly, Ran Balicer, Benjamin Geiger, Yuval Don, and Eran Segal. 2020. A framework for identifying regional outbreak and spread of COVID-19 from one-minute population-wide surveys. *Nature Medicine* (2020). https://doi.org/10.1038/s41591-020-0857-9

[15] Fonnesbeck C Salvatier J., Wiecki T.V. 2016. Probabilistic programming in Python using PyMC3. https://peerj.com/articles/cs-55/

[16] Libin Rong Sha He, Sanyi Tang. 2020. A discrete stochastic model of the COVID-19 outbreak: Forecast and control. , 2792 pages. https://doi.org/10.3934/mbe.2020153

[17] Pedro Teles. 2020. Predicting the evolution of SARS-COVID-2 in Portugal using an adapted SIR model previously used in South Korea for the MERS outbreak. https://arxiv.org/pdf/2003.10047.pdf

A CONVENTIONAL SIR EXAMPLE

As an example, we applied the Bayesian SIR model described to Italy (Figure 2), and obtained $\hat{\beta} = 0.099$, $\hat{\gamma} = 0.0466$, and $R_0 = \hat{\beta}/\hat{\gamma} = 2.12$. We can see from the plot that the total number of cases (purple) is not growing exponentially; therefore, R_0 should be ≤ 1. Instead, we observe $R_0 = 2.12$, which should indicate exponential growth.

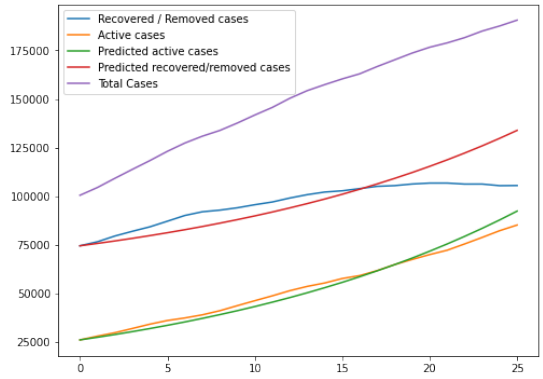

Fig. 2. Fit of conventional SIR model to Italy

B SUPPLEMENTAL PLOTS

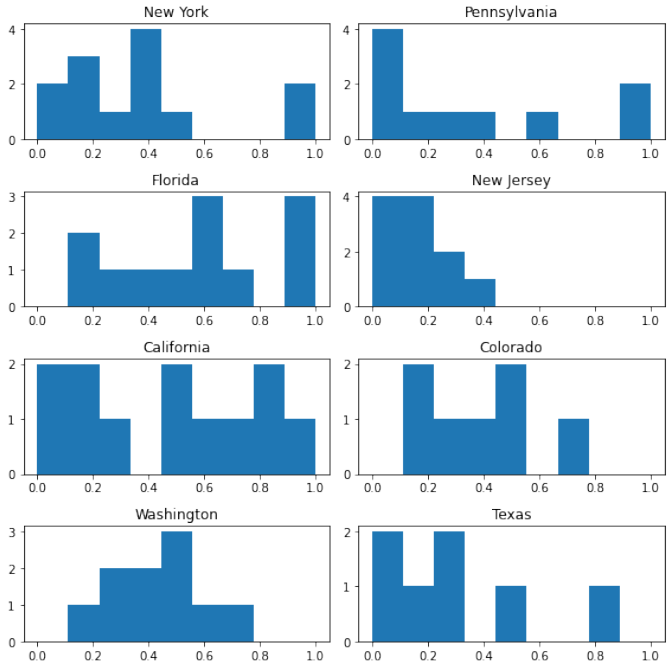

Fig. 3. $F_D(D)$ for States. New Jersey and New York have p-values less than 0.05.

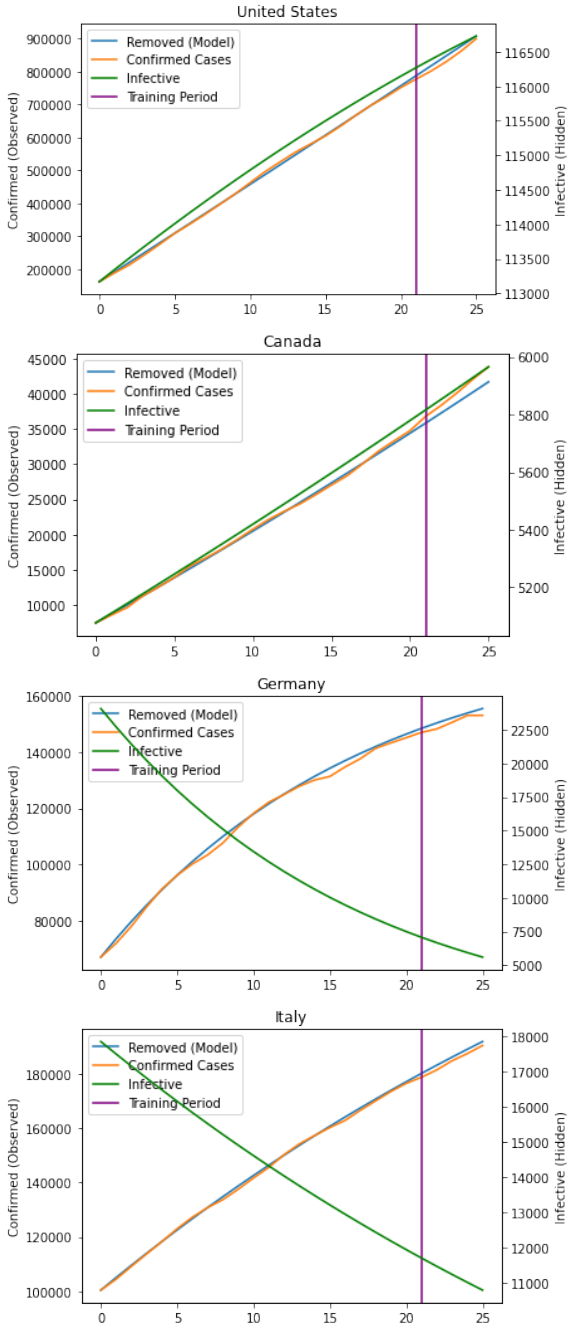

Fig. 4. Sample Mean Estimate for the United States, Canada, Germany, and Italy. Note that confirmed cases and infective cases are on different axes. An infective case curve (green) with increasing slope indicates an overall worsening of the COVID-19 pandemic in that country, and a decreasing slope indicates an overall recovery.

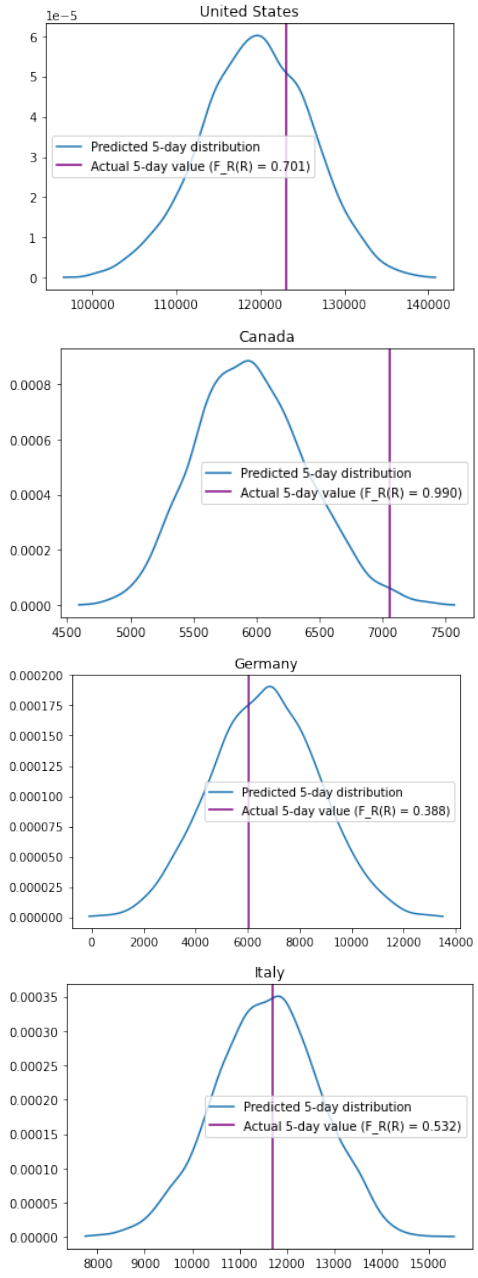

Fig. 5. Country Projection Distribution for the United States, Germany, Canada, and Italy. The purple vertical line indicates the observed value.

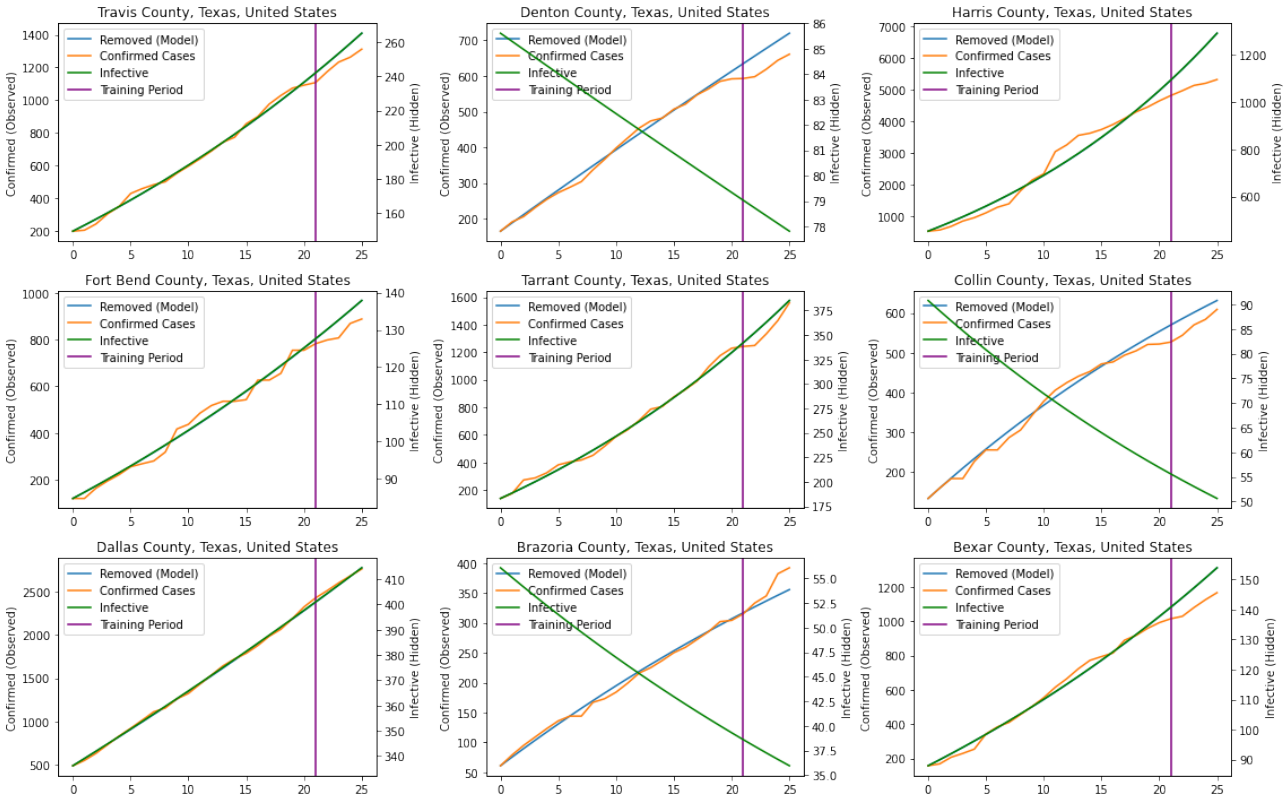

Fig. 6. Sample Mean Estimate for Texas counties. Similarly, note that confirmed cases and infective cases are on different axes. An infective case curve (green) with increasing slope indicates an overall worsening of the COVID-19 pandemic in that country, and a decreasing slope indicates an overall recovery.